

Design for mixing using bubbles in branched microfluidic channels

Piotr Garstecki,^{a)} Michael A. Fischbach, and George M. Whitesides^{b)}

Department of Chemistry and Chemical Biology, Harvard University, 12 Oxford Street, Cambridge, Massachusetts, 02138-2902

(Received 7 December 2004; accepted 4 May 2005; published online 9 June 2005)

This letter describes a method for producing chaotic transport trajectories in planar, microfluidic networks prepared by standard, single-step lithography and operated with a steady-state inflow of the fluids into the device. Gaseous slugs flowing through the network produce temporal variation of pressure distribution and lead to stretching and folding of the continuous fluid. Stabilization of the bubbles by surface-active agents is not necessary, and the method is compatible with the wide range of reactions performed in on-chip bioassays. © 2005 American Institute of Physics.

[DOI: 10.1063/1.1946902]

This letter explores the use of gaseous slugs moving in branching microchannels for formation of unsteady flows that stretch and fold the continuous liquid and cross its laminar streamlines. We show a network of branched channels in which the size of unmixed fluid domains decreases exponentially in the length traveled through the system. The approach is attractive for lab-on-chip applications for four reasons: (i) it does not require multistep lithography for preparation of the devices, (ii) the smallest features it requires are similar in size to the widths of the channels, (iii) it does not involve moving parts or external agitation, and (iv) it is, in principle, compatible with both aqueous and organic fluids.

Typical widths of the channels ($w \sim 100 \mu\text{m}$) and low flow rates ($Q \sim 1 \mu\text{L/s}$) make microfluidics suitable for lab-on-chip applications: on-chip separation,¹ high-throughput screening,² kinetic analysis,³ and formation of gradients for studies of cell response.⁴ Microchannels can be easily fabricated in polymers⁵ and they offer a high degree of control over flows at low and moderate Reynolds (Re) numbers.^{6,7} A perennial problem in microfluidics is mixing.⁸ When $\text{Re} < 1000$, turbulence is absent, and mixing occurs only by diffusion.⁶ Characteristic residence times of the liquid in microfluidic devices are not large enough to ensure homogenization of the reagents by diffusion. Typical Peclet numbers are on the order of $\text{Pe} \approx 10^5$ ($\text{Pe} = Q/wD$, for the diffusion constant $D \approx 10^{-6} \text{cm}^2/\text{s}$) and the liquid would typically have to travel an impractical distance $10^5 w \approx 10 \text{m}$ before diffusion resulted in mixing to homogeneity.

The only available strategy for improved mixing is to boost diffusional transport by enhancing the gradients of concentration. This can be achieved by introducing mixing flows that stretch and fold the liquid and decrease the typical length scales of unmixed streams exponentially in time, which are characteristics of deterministic chaos.⁹ Steady, laminar flow in planar channels is approximately two-dimensional and integrable.¹⁰ Strategies for mixing are based on introduction of either three-dimensional^{7,11} or unsteady¹² flow, and while previous methods have been effective, each has disadvantages: fabrication of passive mixers requires

difficult multistep lithography, while active mixers rely on external agitation and/or moving parts that complicate their design and use.

The use of emulsions provides an attractive way of introducing temporal variations to flow in devices operated at steady-state input. The presence of droplets or bubbles, which we term here slugs, has two important consequences: (i) segmentation of the continuous liquid, which induces recirculation rolls,¹³ and (ii) increased viscous resistance to flow in the capillary or channel.¹⁴ Segmentation of the continuous fluid has been studied as a means to separate liquid domains¹⁵ and as a method to induce recirculatory flow¹⁶ in cylindrical capillaries. Recently, enhancement of mixing by flow segmentation was observed¹⁷ and applied to microfluidic systems for gas-liquid¹⁸ and liquid-liquid^{3,19} dispersions.

Here we extend this methodology by designing a mixer based on the second property of slug flow: increased resistance. Slugs traveling through the arms of a network of branched channels provide temporal variation in the distribution of pressures between the branches. This pressure differential leads to crossing of laminar streamlines of the continuous liquid and to exponential stretching and folding of the interface between the two unmixed streams.

We form bubbles²⁰ in a flow focusing (FF) geometry [Fig. 1(a)] prepared in poly(dimethylsiloxane).⁵ The FF region [Fig. 1(a)] comprises two inlet channels for the two liquid streams (water/glycerol/Tween20 solutions delivered from a syringe pump, Harvard Apparatus PhD2000) and a single inlet channel for the gaseous phase (nitrogen from a pressurized tank). The gaseous thread periodically enters the orifice, breaks, and releases bubbles into the outlet channel. The volume of the bubble and the volume fraction of the

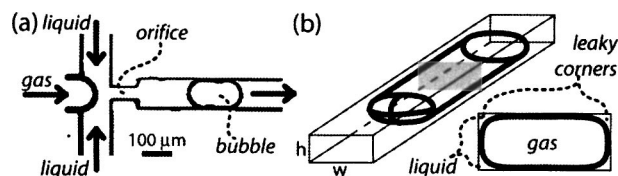


FIG. 1. (a) An optical micrograph of the flow focusing device. We deliver the continuous liquid from the two side inlets and the gas from the center inlet channel. The gaseous thread periodically releases bubbles into the outlet channel. (b) Schematic illustrations of an immiscible plug in a rectangular capillary. The gas-liquid interface is marked with the thick solid line, and the walls of the channel with a thin solid line.

^{a)}Electronic mail: pgarstecki@gmwhgroup.harvard.edu

^{b)}Electronic mail: gwhitesides@gmwhgroup.harvard.edu

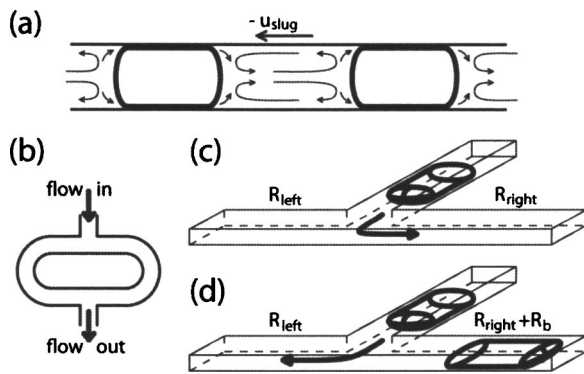


FIG. 2. (a) Schematic illustration of the streamlines of the continuous fluid in a reference frame traveling at the speed u_{slug} of the slug (the walls travel at $-u_{\text{slug}}$ and the plugs are stationary). Portion of the host fluid bypasses the bubble through the corners of the capillary; the remaining part recirculates and forms convection rolls. (b) A single unit of the bubble micromixer—a channel that branches and recombines. (c) Bubble coming to the branching units chooses the arm characterized by the lower resistance. The bubble increases the resistance of the channel and the following plug flows into the opposite arm (d).

gaseous phase can be controlled by adjusting the pressure p applied to the gas stream and the total rate of flow Q of the two liquid streams. We use the two inlets for the continuous fluid to supply the liquids to be mixed. In most experiments, the liquids contained 2% (w/w) Tween20 surfactant, and for visualization purposes, one of the liquids contained dye (Waterman black ink). The flow rates of the transparent liquid q_t and the black liquid q_b were equal: $q_t = q_b = Q/2$.

Large parts of the surface of the slug are separated from the wall of the channel only by a thin wetting film of the continuous fluid, and the slug does not fill the cross section of the channel entirely¹⁴ [Fig. 1(b)]. The thin films of liquid between the slug and the walls of the channel lead to increased viscous dissipation and the speed u_{slug} of the slug does not match the mean velocity $u_{\text{mean}} = Q/A$ of the host fluid. There are two consequences of this disparity. First, the flow of the continuous fluid can be divided into two contributions: the “slug” flow Q_{slug} , which is flow at a mean velocity of the slug, $Q_{\text{slug}} = Au_{\text{slug}}$; and the flow in the “leaky” corners $Q_{\text{corner}} = Q - Q_{\text{slug}}$. The portion of the continuous fluid that is confined between the slugs develops convection rolls [Fig. 2(a)] which were previously used for mixing.^{3,16,18,19} Here, we exploit the second property of slug flow—increased resistance to flow—to mix the continuous fluid. Our system comprises a single channel interrupted by “units” of two channels running in parallel [Fig. 2(b)]. For a Newtonian fluid, the resistance R_S to flow in capillaries at low to moderate Reynolds number is described by the Hagen-Poiseuille equation, $R_S = \Delta p / Q$, where Δp is the pressure drop along the capillary of length L . R_S depends on the viscosity μ of the fluid and on the hydrodynamic radius r_h of the channel ($R_S = \mu L / r_h^4$ for capillaries of nearly-square cross section, $r_h \approx w$). The pressure drop per unit length Δp^* is a function of the externally controlled flow rate and the resistance of the channel, $\Delta p^* = R_S Q / L$. A slug introduced into a rectangular capillary increases its resistance to flow,¹⁴ and the pressure drop across the length l_b of the bubble is larger than $l_b \Delta p^*$. We can associate the presence of the bubble in a capillary with a positive contribution to its resistance, $R = R_S + nR_b$, where R_b is the effective increase in resistance per bubble and n is the number of bubbles in the capillary.

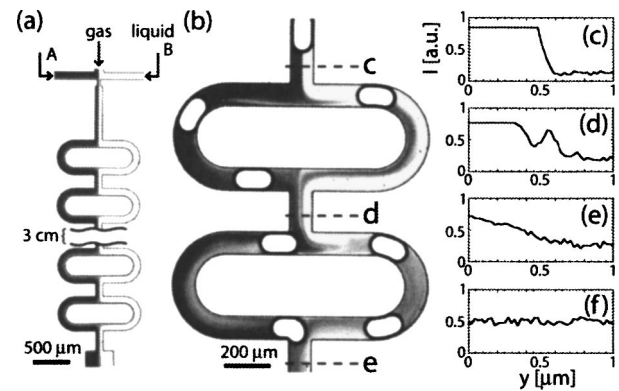


FIG. 3. Optical micrographs of the micromixer. (a) Laminar flow without bubbles. (b) Plugs flowing through the network. In the first branching section, there are two bubbles in the left arm and one bubble in the right arm. The lower resistance in the right arm redirects a portion of the black liquid into the right (originally clear) channel. The dashed lines mark the positions at which we measured the intensity profile across the width of the channel. Normalized intensity profiles are shown in insets (c)–(f), with the last profile—which indicates homogeneous distribution of the dye in the channel—measured after the sixth unit.

In the simplest design [Fig. 2(b)] of the mixer the two parallel channels have equal lengths and cross sections; and their resistances are equal $R_{\text{left}}(n=0) \approx R_{\text{right}}(n=0)$. The pressure drop along each arm is the same, and so are the rates of inflow of the liquid into the two arms: $q_{\text{left}}/q_{\text{right}} = R_{\text{right}}/R_{\text{left}} \approx 1$. When a bubble reaches the junction, it flows into the arm characterized by lower resistance,^{21,22} [the right channel in Fig. 2(c)]. The presence of the bubble increases resistance to flow in the right channel $R_{\text{right}} = R_{\text{right}}(0) + R_b$, and the next bubble flows into the left arm [Fig. 2(d)]. The system exhibits *memory*; bubbles remaining in the branching region “encode” the resistances of the two parallel arms.²³

Figure 3(a) shows a micrograph of the micromixer. In the absence of bubbles, the two streams (black and clear) repeatedly split into the left and right arms ($q_{\text{left}} = q_{\text{black}}$, and $q_{\text{right}} = q_{\text{clear}}$) and recombine, flowing laminarly without significant broadening of the interface. When we introduce slugs into the network [Fig. 3(b)], the resistances of the channels in each parallel set are no longer equal. If there are more bubbles in the left channel, $R_{\text{left}} > R_{\text{right}}$, so that less liquid flows into the left channel: $q_{\text{left}}/q_{\text{right}} = R_{\text{right}}/R_{\text{left}} < 1$. Since the black and clear liquids are supplied at equal rates, some of the black liquid flows into the right (originally entirely clear) arm. The ratio of the resistances in the parallel channels changes each time a bubble enters or leaves the unit, so the system periodically sends volumes of black liquid into the clear arm and vice versa. This oscillation of the inflow of each stream into the arms stretches and folds the interface between the clear and black liquids. The color distribution across the single channel after the first mixing unit [Fig. 3(d)] shows two distinctive maxima, which indicates crossing of the streamlines of the continuous fluid.

In order to assess whether the flow satisfies the criteria⁹ of a properly designed mixer, we perform the following estimate and we verify it by quantifying the concentration profiles along the channel. We postulate that each branching unit doubles the area of interface between the two liquids and the overall increase is exponential in the distance traveled downstream. We estimate the number of units needed to mix the two liquids by comparing the average

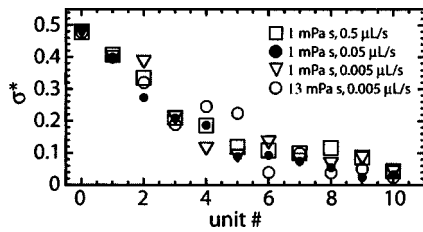


FIG. 4. Standard deviation of the intensity profile as a function of position along the channel network. Unit index equal to zero corresponds to the profile obtained upstream of the first unit [as in Fig. 2(c)]. $\sigma^* = 0.5$ signifies unmixed streams, while $\sigma^* = 0$ corresponds to fully homogenized liquid. Behavior of the system does not change over a wide range of the rates of flow $Q \in (5 \times 10^{-3}, 0.5) \mu\text{L/s}$ and viscosity $\mu \in (1, 13) \text{ mPa s}$ of the host fluid. This is consistent with the model assuming exponential increase of the area of interface between the two liquid streams. The volume fraction of the slugs in the network was $\phi \approx 0.5, 0.2, 0.15,$ and 0.2 for $Q = 0.5, 0.05, 0.005 \mu\text{L/s}$ ($\mu = 0.9 \text{ mPa s}$) and $Q = 0.005 \mu\text{L/s}$ ($\mu = 13 \text{ mPa s}$), respectively.

distance between two black-clear interfaces $d_{\text{inter}} \sim w2^{-l/a}$ (where l is the length traveled downstream and a is the arc length of the arm in the branching section) and the diffusional length scale $d_{\text{diff}} = (tD)^{1/2}$ (with time t related to distance $l = tQ/w^2$ traveled downstream). We assume mixing to homogeneity at distance l_{mix} at which $d_{\text{inter}} = d_{\text{diff}}$, leading to $l_{\text{mix}}/a = (2 \ln 2)^{-1} [\ln \text{Pe} - \ln(l_{\text{mix}}/w)]$ with $\text{Pe} = Q/Dw = 10^5$ for $Q = 1 \mu\text{L/s}$, $D = 10^{-6} \text{ cm}^2/\text{s}$, and $w = 100 \mu\text{m}$. If we neglect the term $\ln(l_{\text{mix}}/w)$, which is small in comparison to $\ln \text{Pe}$, we obtain $l_{\text{mix}}/a \approx 8$. In accordance with the assumption of exponential folding, this prediction (l_{mix}/a) is largely insensitive to the initial value of the Peclet number: $l_{\text{mix}}/a \approx 7$ for $\text{Pe} = 10^4$ and $l_{\text{mix}}/a \approx 10$ ($\text{Pe} = 10^6$).

We performed experiments with a range of flow rates, $Q \in (5 \times 10^{-3}, 0.5) \mu\text{L/s}$, and two different viscosities of the host fluid $\mu \in (0.9, 13) \text{ mPa s}$. We measured the intensity profiles $I(y)$ of light across the channel after each mixing unit [Figs. 3(c)–3(f)], and we quantified mixing by dividing the standard deviation of $I(y)$ by its mean value: $\sigma^* = \sigma[I(y)]/\langle I(y) \rangle$. A value of $\sigma^* = 0.5$ indicates unmixed streams, and $\sigma^* = 0$ signifies complete mixing. In agreement with our estimates, we observe homogenization of the two aqueous streams within ten branching units. The system behaves similarly over the whole range of Reynolds [$\text{Re} \in (10^{-2}, 10^2)$] and Peclet [$\text{Pe} \in (10^3, 10^6)$] numbers tested in our experiments (Fig. 4). These results confirm our assumption of exponential folding of the liquid domains, and they demonstrate the efficiency⁹ of our branched channel mixer. We observe that the device mixes efficiently for volume fractions of the gaseous phase $\phi > 0.1$, below which value mixing efficiency drops substantially.

We have presented a design for mixing adjacent streams in branched microfluidic channels that uses gaseous slugs

to create unsteady flow conditions in a planar microchannel network. This mixing strategy is simple, and has the potential to be used for the design of simple micromixers for cost-effective lab-on-chip applications.

One of the authors (P.G.) acknowledges support of the Foundation for Polish Science. Another (M.A.F.) acknowledges support from the Hertz Foundation. This work was supported in part by the U.S. Department of Energy under award DE-FG02-OOER45852 and in part by the National Institutes of Health (NIGMS) under award GM065364. We thank the Harvard MRSEC for the use of facilities.

- ¹H. Lu, S. Gaudet, M. A. Schmidt, and K. F. Jensen, *Anal. Chem.* **76**, 5705 (2004); Y. H. Dou, N. Bao, J. J. Xu, F. Meng, and H. Y. Chen, *Electrophoresis* **25**, 3024 (2004).
- ²C. L. Hansen, M. O. A. Sommer, and S. R. Quake, *Proc. Natl. Acad. Sci. U.S.A.* **101**, 14431 (2004); B. Zheng, L. S. Roach, and R. F. Ismagilov, *J. Am. Chem. Soc.* **125**, 11170 (2003).
- ³H. Song and R. F. Ismagilov, *J. Am. Chem. Soc.* **125**, 14613 (2003).
- ⁴S. K. W. Dertinger, X. Y. Jiang, Z. Y. Li, V. N. Murthy, and G. M. Whitesides, *Proc. Natl. Acad. Sci. U.S.A.* **99**, 12542 (2002).
- ⁵D. C. Duffy, J. C. McDonald, O. J. A. Schueller, and G. M. Whitesides, *Anal. Chem.* **70**, 4974 (1998); J. C. McDonald, D. C. Duffy, J. R. Anderson, D. T. Chiu, H. K. Wu, O. J. A. Schueller, and G. M. Whitesides, *Electrophoresis* **21**, 27 (2000).
- ⁶P. J. A. Kenis, R. F. Ismagilov, and G. M. Whitesides, *Science* **285**, 83 (1999).
- ⁷A. D. Stroock, S. K. W. Dertinger, A. Ajdari, I. Mezic, H. A. Stone, and G. M. Whitesides, *Science* **295**, 647 (2002).
- ⁸M. A. Stremler, F. R. Haselton, and H. Aref, *Philos. Trans. R. Soc. London, Ser. A* **362**, 1019 (2004).
- ⁹J. M. Ottino and S. Wiggins, *Science* **305**(5683), 485 (2004).
- ¹⁰E. Lauga, A. D. Stroock, and H. A. Stone, *Phys. Plasmas* **16**, 3051 (2004).
- ¹¹R. H. Liu, M. A. Stremler, K. V. Sharp, M. G. Olsen, J. G. Santiago, R. J. Adrian, H. Aref, and D. J. Beebe, *J. Microelectromech. Syst.* **9**, 190 (2000).
- ¹²F. Okkels and P. Tabeling, *Phys. Rev. Lett.* **92**, 038301 (2004); V. Studer, G. Hang, A. Pandolfi, M. Ortiz, W. F. Anderson, and S. R. Quake, *J. Appl. Phys.* **95**, 393 (2004).
- ¹³G. I. Taylor, *J. Fluid Mech.* **10**, 161 (1961).
- ¹⁴H. Wong, C. J. Radke, and S. Morris, *J. Fluid Mech.* **292**, 71 (1995).
- ¹⁵L. R. Snyder and H. J. Adler, *Anal. Chem.* **48**, 1017 (1976).
- ¹⁶L. R. Snyder and H. J. Adler, *Anal. Chem.* **48**, 1022 (1976).
- ¹⁷M. A. Burns, C. H. Mastrangelo, T. S. Sammarco, F. P. Man, J. R. Webster, B. N. Johnson, B. Foerster, D. Jones, Y. Fields, A. R. Kaiser, and D. T. Burke, *Proc. Natl. Acad. Sci. U.S.A.* **93**, 5556 (1996).
- ¹⁸A. Gunther, S. A. Khan, M. Thalmann, F. Trachsel, and K. F. Jensen, *Lab Chip* **4**, 278 (2004).
- ¹⁹J. R. Burns and C. Ramshaw, *Lab Chip* **1**, 10 (2001).
- ²⁰P. Garstecki, I. Gitlin, W. DiLuzio, E. Kumacheva, H. A. Stone, and G. M. Whitesides, *Appl. Phys. Lett.* **85**, 2649 (2004).
- ²¹A bubble can also break at the junction. This complicates the description but yields similarly efficient mixing.
- ²²D. R. Link, S. L. Anna, D. A. Weitz, and H. A. Stone, *Phys. Rev. Lett.* **92**, 054503 (2004).
- ²³A more detailed description of the dynamics of bubble movement in networks of microfluidic channels will be presented elsewhere; M. J. Fuerstman, P. Garstecki, and G. M. Whitesides (unpublished).